Comparison of shallow firn core records from Quelccaya Ice Cap (Peru) and Nevado Illimani (Bolivia) and potential for future ultra-high-resolution investigation

Heather M. Clifford[1,2], Mariusz Potocki[1,2], Charles Rodda[1,2], Daniel Dixon[1], Sean Birkel[1,2], Michael Handley[1], Elena Korotkikh[1], Franciele Schwanck[3], Flavia A. Tavares[3], Ronaldo T. Bernardo[3], Filipe G. L. Lindau[3], Oscar Vilca Gomez[4,5,6], Harrison Jara-Infantes[5], Victor Bustínza Urviola[5], L. Baker Perry[7], Jonathan Maurer[2], Anton Seimon[7], Margit Schwikowski[8], Gino Casassa[9], Shugui Hou[10,11], Andrei V. Kurbatov[1,2], Kimberley R. Miner[1], Jefferson C. Simões[1,3], Paul A. Mayewski[1,2]

1. Climate Change Institute, University of Maine, Orono, Maine, USA
2. School of Earth and Climate Sciences, University of Maine, Orono, Maine, USA
3. Centro Polar e Climático, Universidade Federal do Rio Grande do Sul, Porto Alegre, Brazil
4. Unidad de Glaciología y Recursos Hídricos. Autoridad Nacional de Agua. Huaraz, Perú
5. National Research Institute for Glaciers and Mountain's Ecosystems (INAIGEM), Huaraz, Peru
6. Programa de Maestría en Recursos Hídricos, Universidad Nacional Agraria La Molina, Lima, Perú
7. Department of Geography and Planning, Appalachian State University, Boone, NC, USA
8. Paul Scherrer Institute, Villigen, Switzerland
9. Centro de Investigación Gaia Antártica, Universidad de Magallanes, Punta Arenas, Chile
10. School of Geography and Ocean Science, Nanjing University, Nanjing, China
11. School of Oceanography, Shanghai Jiao Tong University, Shanghai, China.

Supplementary Materials

Figure S1. The 7-m near basal ice core from the edge of the Quelccaya ice cap (QNB-18, 13.939975S, -70.856443W, ~5245-m), was collected from the top of the glacier section shown in this image, located about 5-km from QU-18. This sampling location was chosen since layering was visible in the basal ice, as seen in this image.

Table S1. Summary of statistics from Quelccaya and Illimani IC and ICP-MS blank values and detection limits.

|	Quelccaya Blanks (n=14)		Illimani Blanks (n=20)		Instrumental Detection Limits
	mean	std	mean	std	
ug/L					
Na^+	4.2	3.3	7.7	6.4	0.3
K^+	0.8	0.6	2.0	1.5	0.1
Mg^{2+}	2.1	1.0	5.9	0.8	0.1
Ca^{2+}	34.6	31.3	31.7	18.3	0.3
Cl^-	9.6	5.1	15.0	6.5	0.3
NO_3^-	9.7	4.3	14.9	1.7	0.2
SO_4^{2-}	75.2	39.9	45.3	25.6	1.2
Al	19.0	31.6	2.1	2.7	0.0
S	11.0	3.6	3.9	7.7	0.3
Ca	6.7	7.9	11.4	11.0	0.1
Mn	0.3	0.4	0.6	0.7	0.0
Fe	16.1	25.5	5.5	7.1	0.0
Na	17.4	9.3	3.8	4.1	
Mg	1550.4	1381.8	3.9	3.9	
Cu	0.1	0.1	0.1	0.1	0.0
Zn	0.6	0.7	0.7	1.0	
Si	55.9	75.8	55.5	33.4	
K	7.7	10.4	5.8	6.3	
ng/L					
Sr	91.0	131.9	139.6	151.3	0.3
Cd	0.3	0.2	1.5	1.3	0.0
Cs	4.2	5.8	1.9	2.2	0.0
Ba	47.3	55.0	234.3	246.1	0.3
La	1.2	1.8	0.7	0.8	
Ce	3.0	4.6	1.4	1.5	
Pr	0.3	0.5	0.2	0.2	
Pb	70.1	76.0	17.7	24.4	0.2
Bi	0.3	0.2	0.4	0.4	0.0
U	2.7	3.3	0.2	0.2	0.0
As	15.0	20.1	26.7	26.0	
Li	69.2	120.6	18.4	3.9	
Sc	1.9	1.7	2.3	0.2	
Ag	2.0	1.8	0.6	0.2	
Ti	1671.2	2787.1	513.5	968.6	0.7
V	24.1	34.9	10.4	12.9	0.1
Cr	18.8	23.7	7.4	5.3	0.1
Co	7.2	10.2	7.6	8.7	0.4
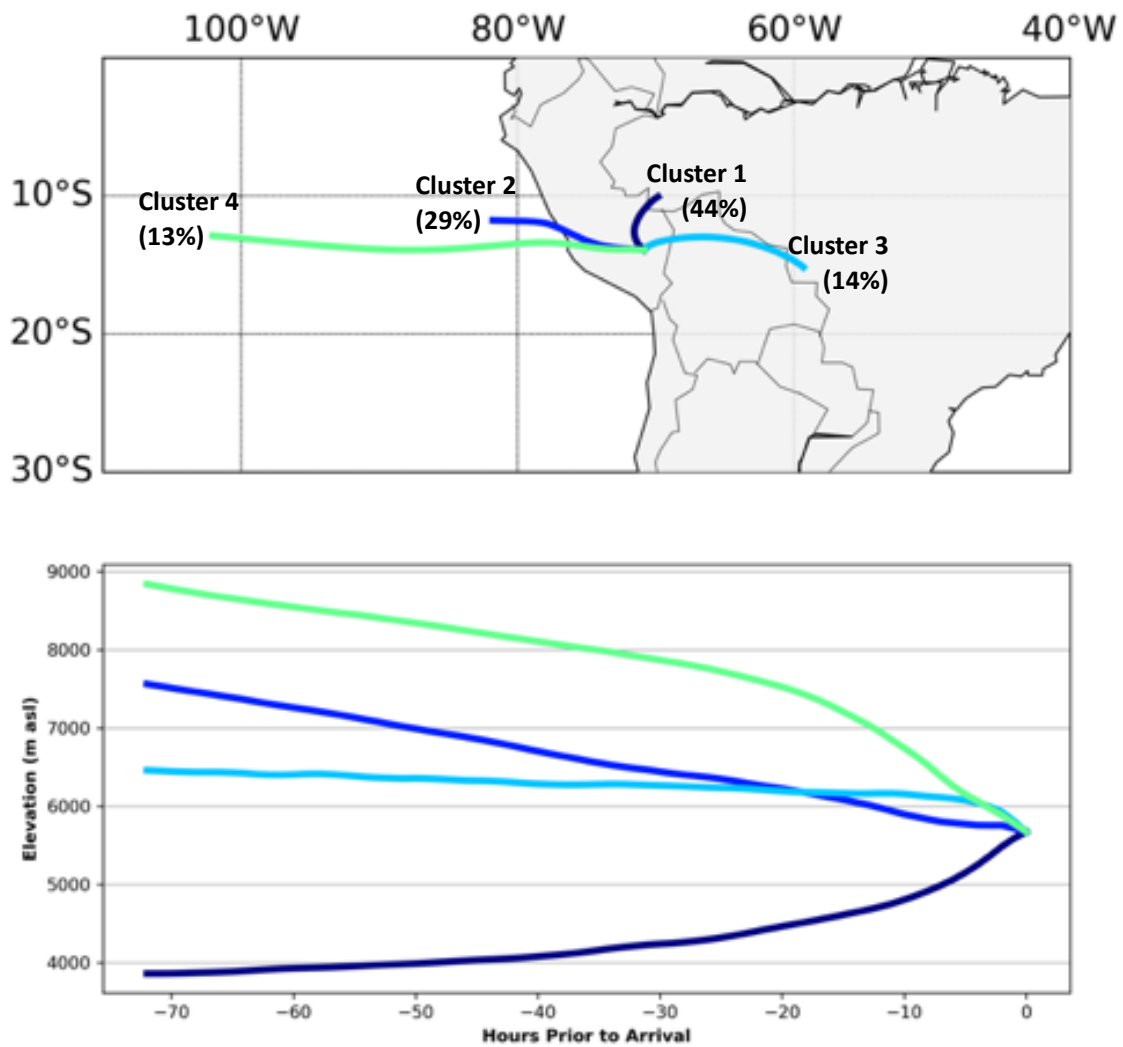
Figure S2. NOAA HYSPLIT back trajectory results for the 2013 full year GDAS dataset, originating from the summit of the Quelccaya Ice Cap. Methodology for the HYSPLIT back trajectory analysis is detailed in the methodology section 2.4.
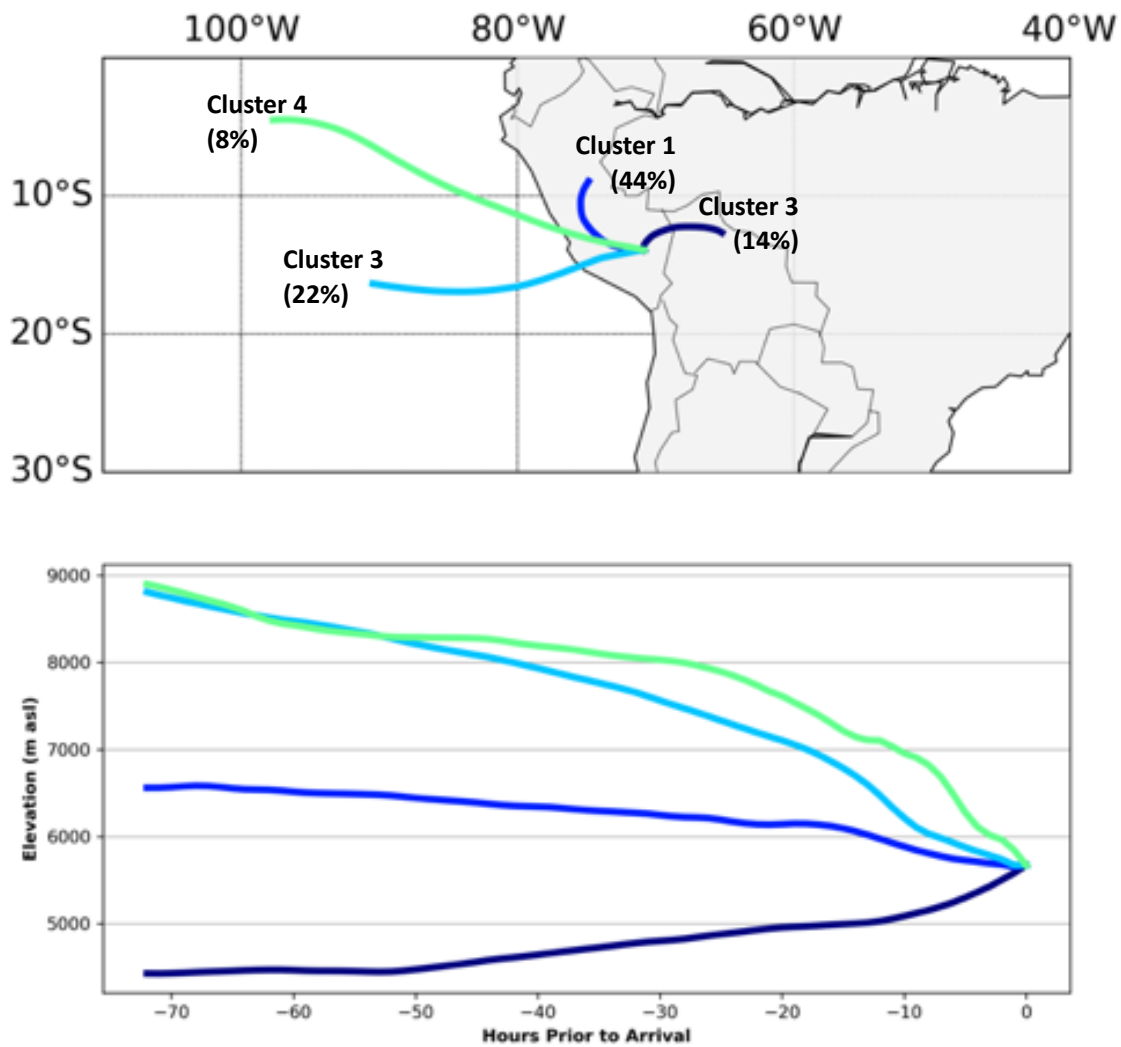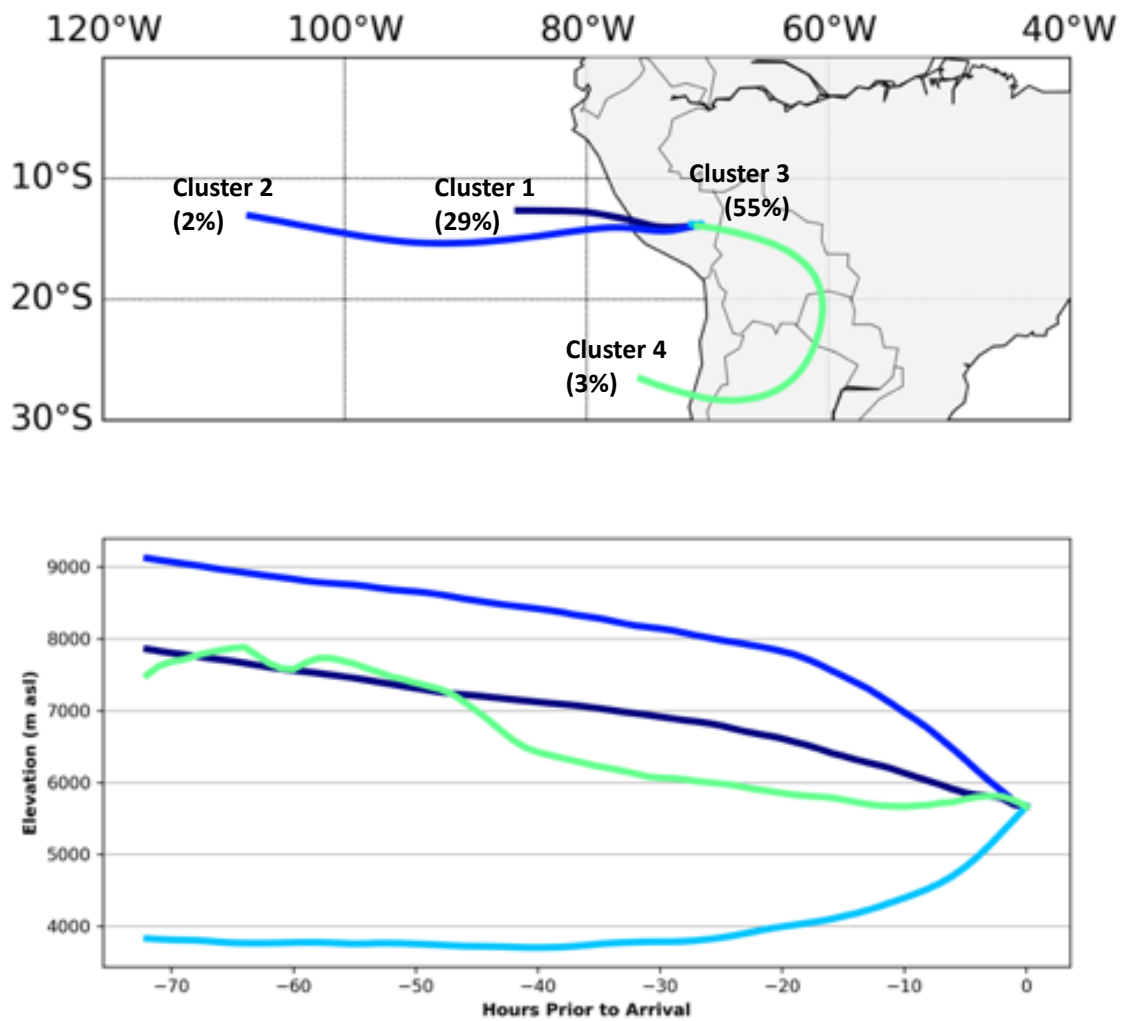
Figure S3. NOAA HYSPLIT back trajectory results for 2013 Autumn (MAM) GDAS dataset, originating from the summit of the Quelccaya Ice Cap. Methodology for the HYSPLIT back trajectory analysis is detailed in the methodology section 2.4.
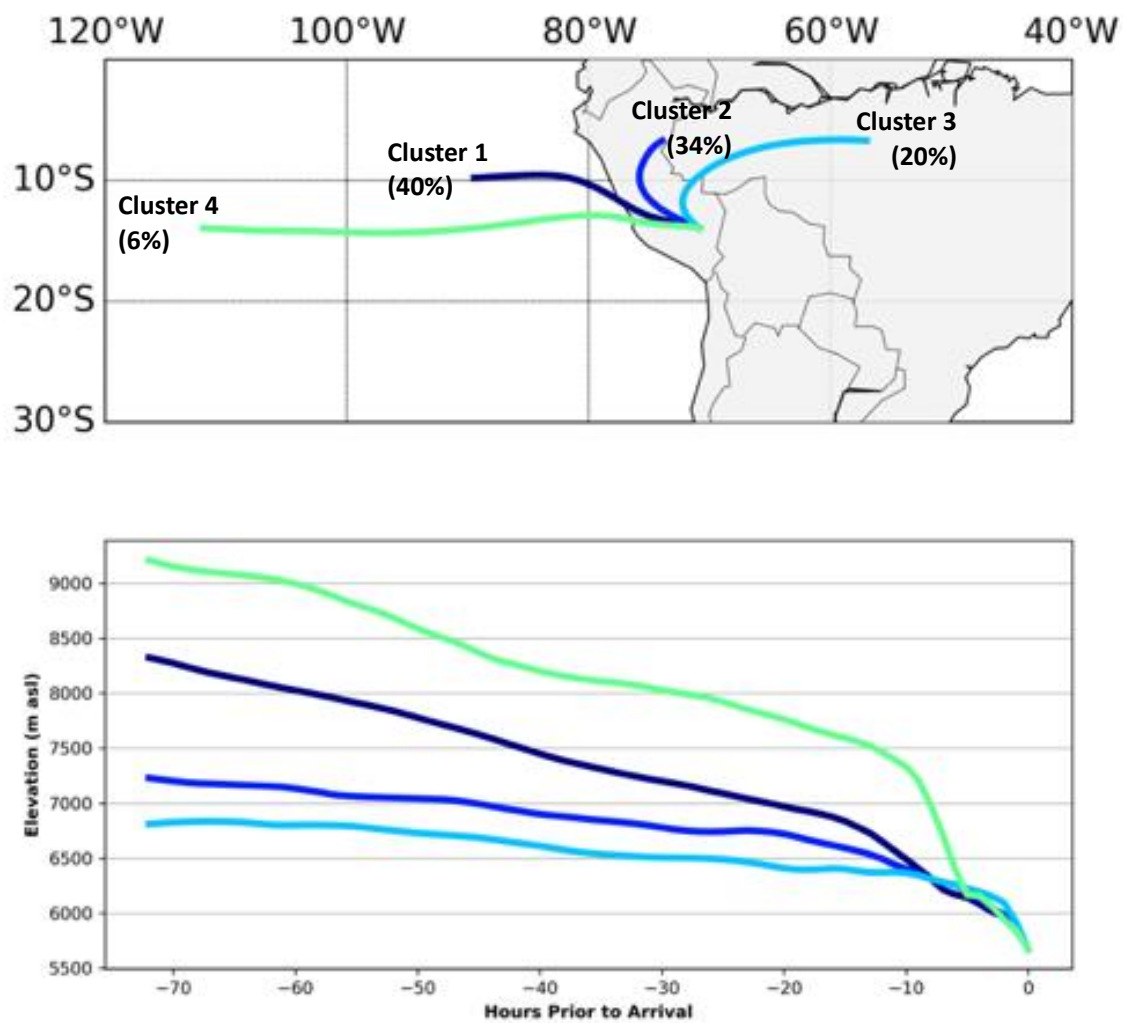
Figure S4. NOAA HYSPLIT back trajectory results for 2013 Winter (JJA) GDAS dataset, originating from the summit of the Quelccaya Ice Cap. Methodology for the HYSPLIT back trajectory analysis is detailed in the methodology section 2.4.
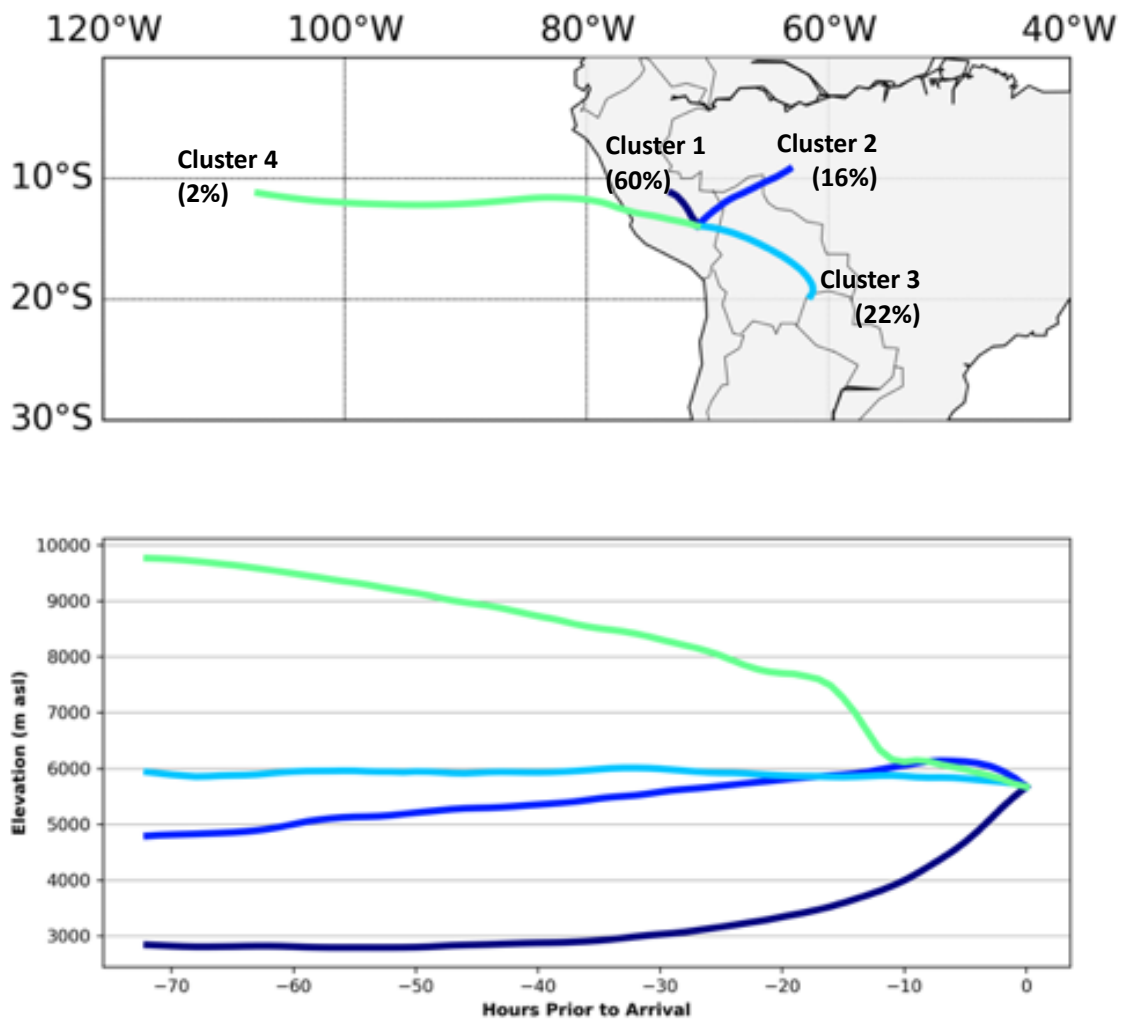
Figure S5. NOAA HYSPLIT back trajectory results for 2013 Summer (DJF) GDAS dataset, originating from the summit of the Quelccaya Ice Cap. Methodology for the HYSPLIT back trajectory analysis is detailed in the methodology section 2.4.

Figure S6. NOAA HYSPLIT back trajectory results for 2013 Spring (SON) GDAS dataset, originating from the summit of the Quelccaya Ice Cap. Methodology for the HYSPLIT back trajectory analysis is detailed in the methodology section 2.4.
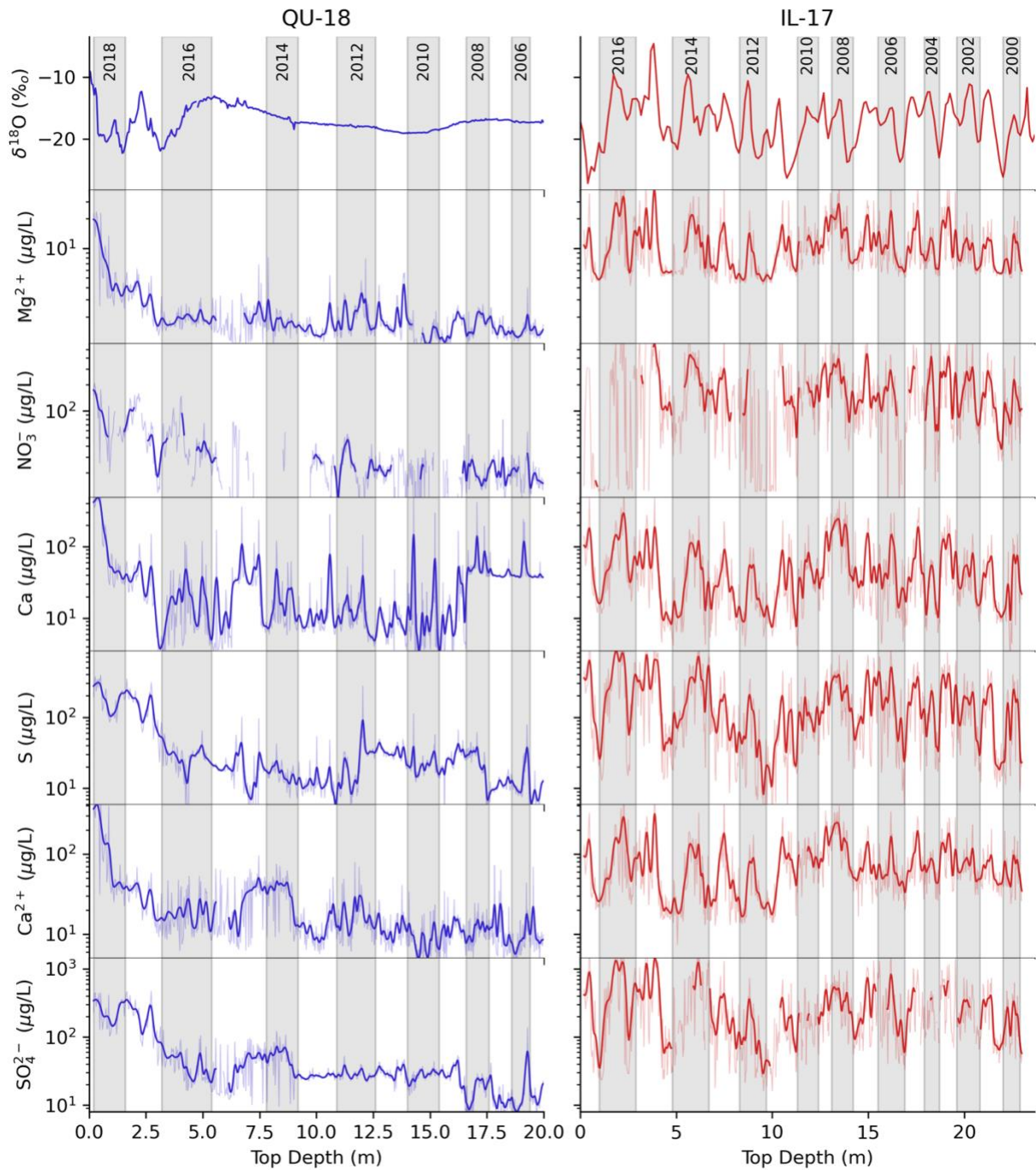
Figure S7. Raw and smoothed (1σ gaussian) glaciochemistry ($\delta^{18}O$, Mg^{2+}, NO_3^-, Ca, S, Ca^{2+}, SO_4^{2-}) measurements from QU-18 (left, blue) and IL-17 short core (right, red) by depth in meters. The vertical highlights indicate where the years are located by depth from annual layer counting (QU-18) and from Lindau and others, 2020 (IL-17).
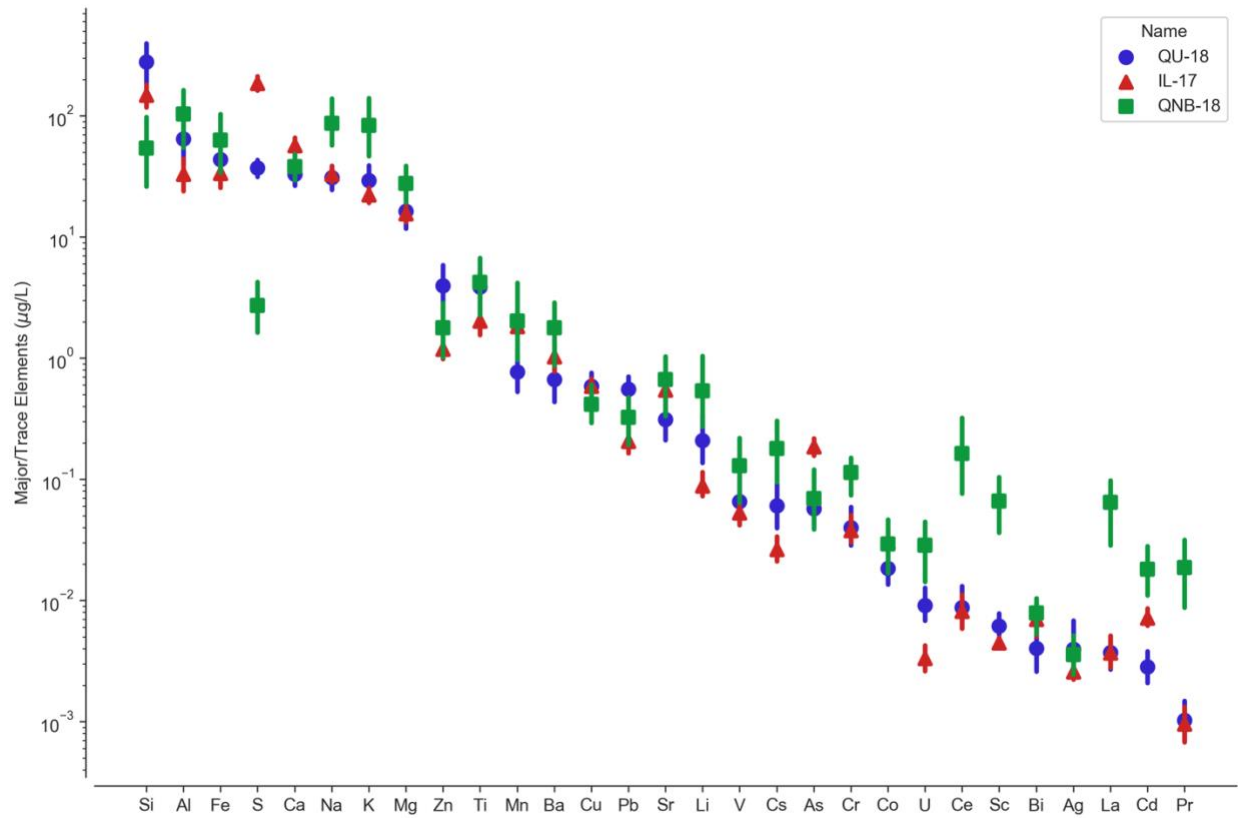
Figure S8. Statistical overview (mean, ci=0.95) of major and trace element concentrations for the entirety of QU-18 (blue circle), IL-17 (red triangle) shallow firn cores, and the old Quelccaya near basal ice QNB-18 (green square).
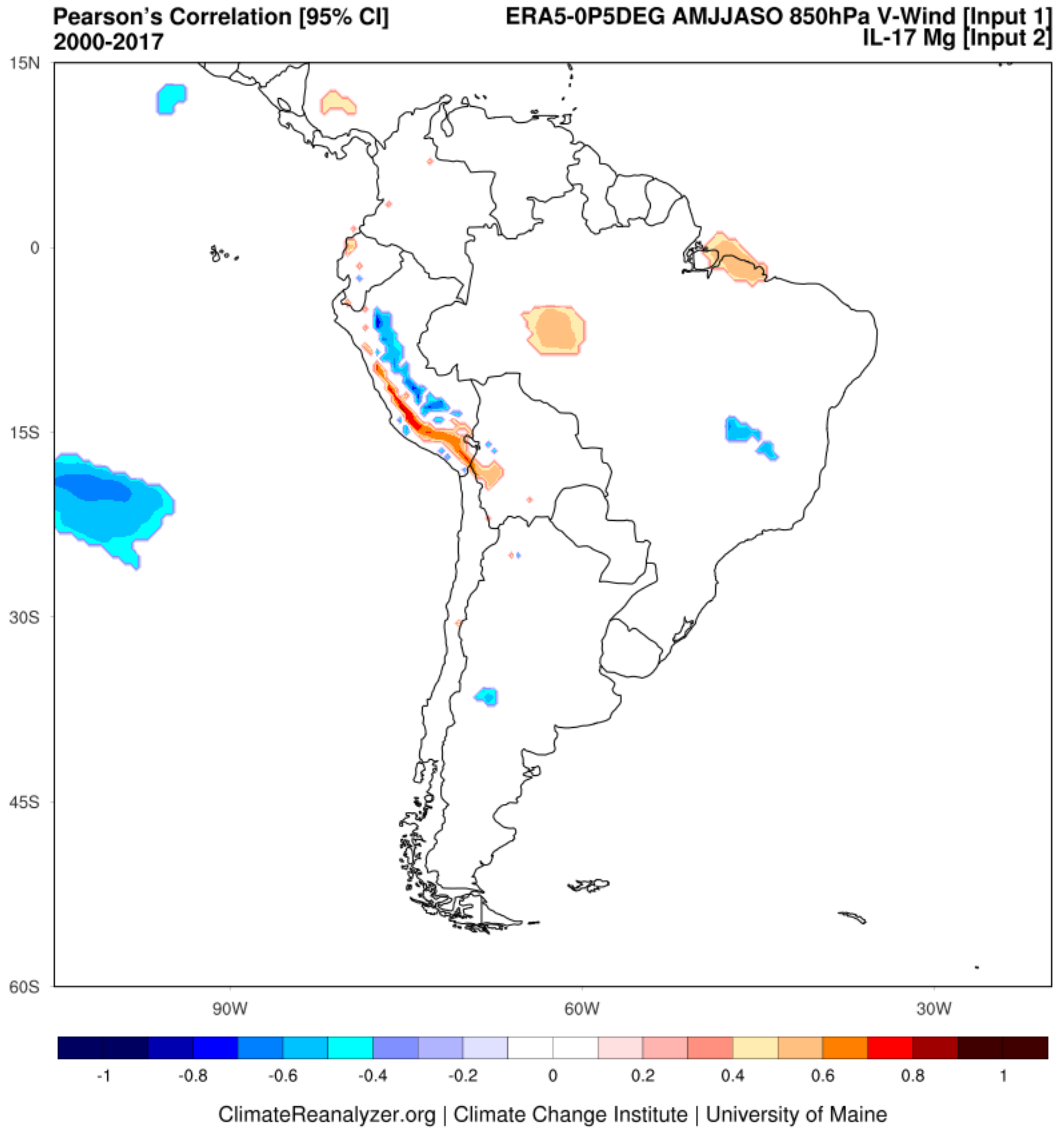
Figure S9. Pearson's correlation (95% CI) of ERA5 AMJJASO 850hPa V-wind to IL-17 Mg record from 2000 to 2017. This map was generated by the University of Maine's Climate Change Institute data-visualization website Climate Reanalyzer (https://climatereanalyzer.org).
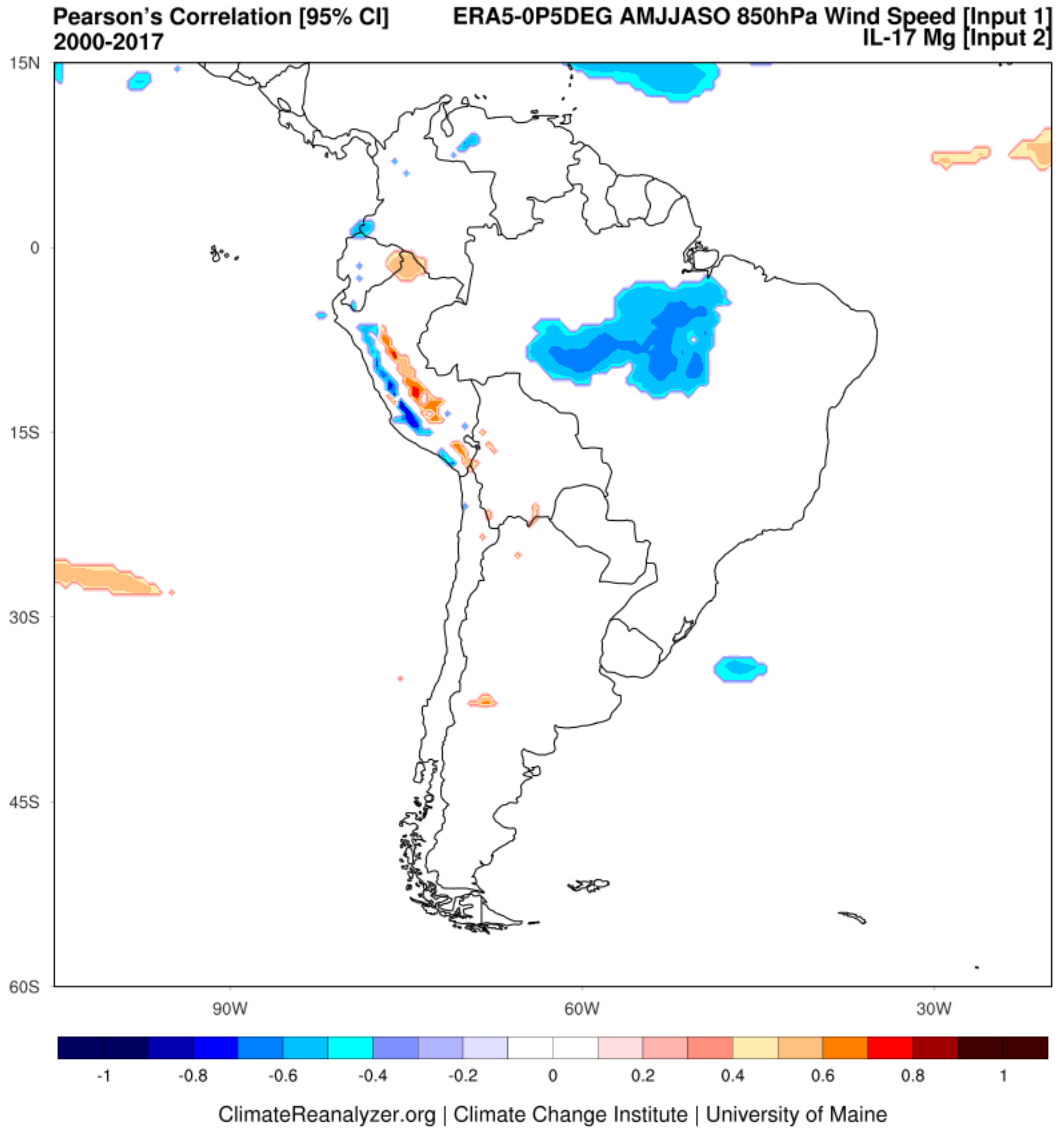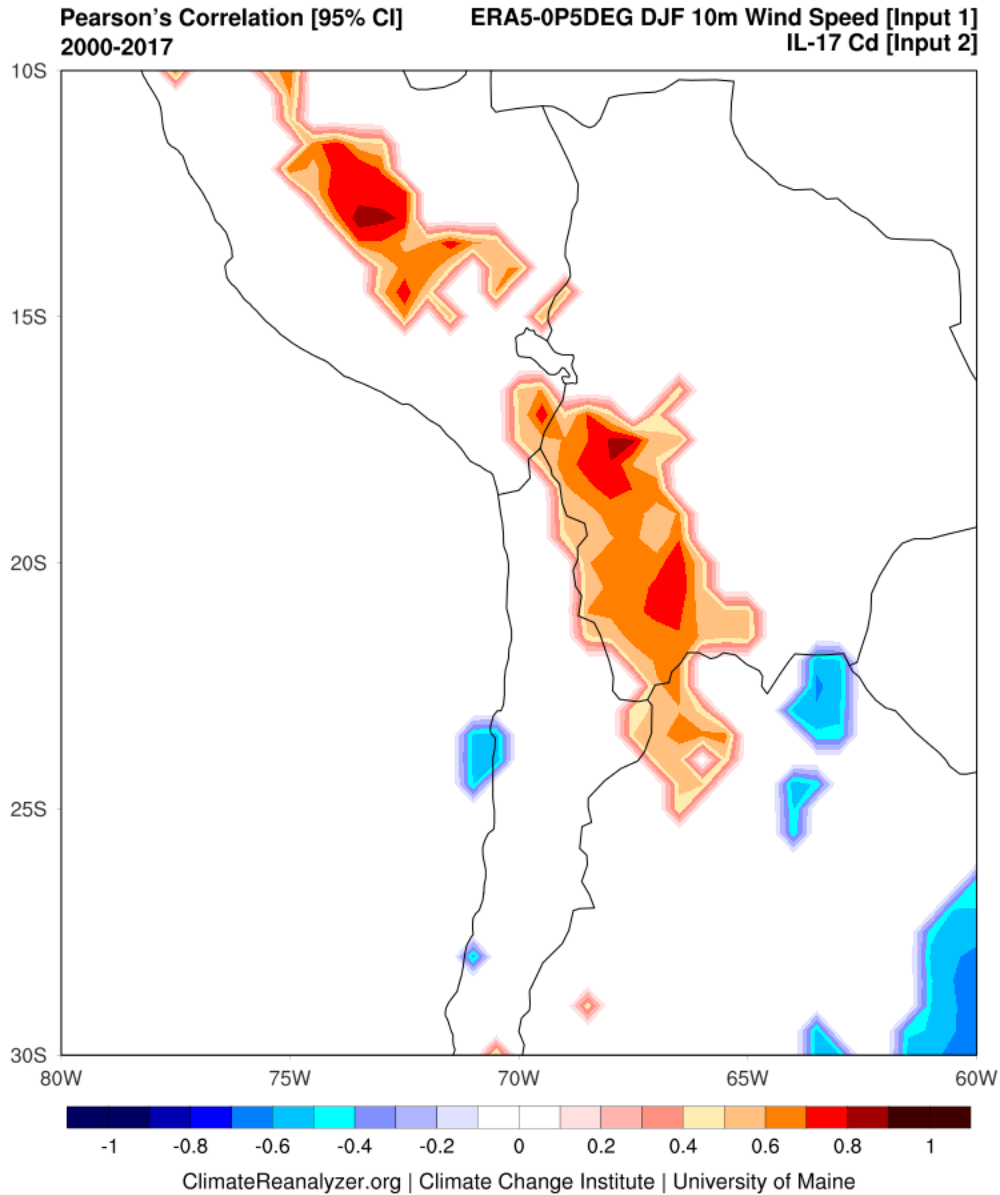
Figure S10. Pearson's correlation (95% CI) of ERA5 AMJJASO 850hPa wind speed to IL-17 Mg record from 2000 to 2017. This map was generated by the University of Maine's Climate Change Institute data-visualization website Climate Reanalyzer (https://climatereanalyzer.org).
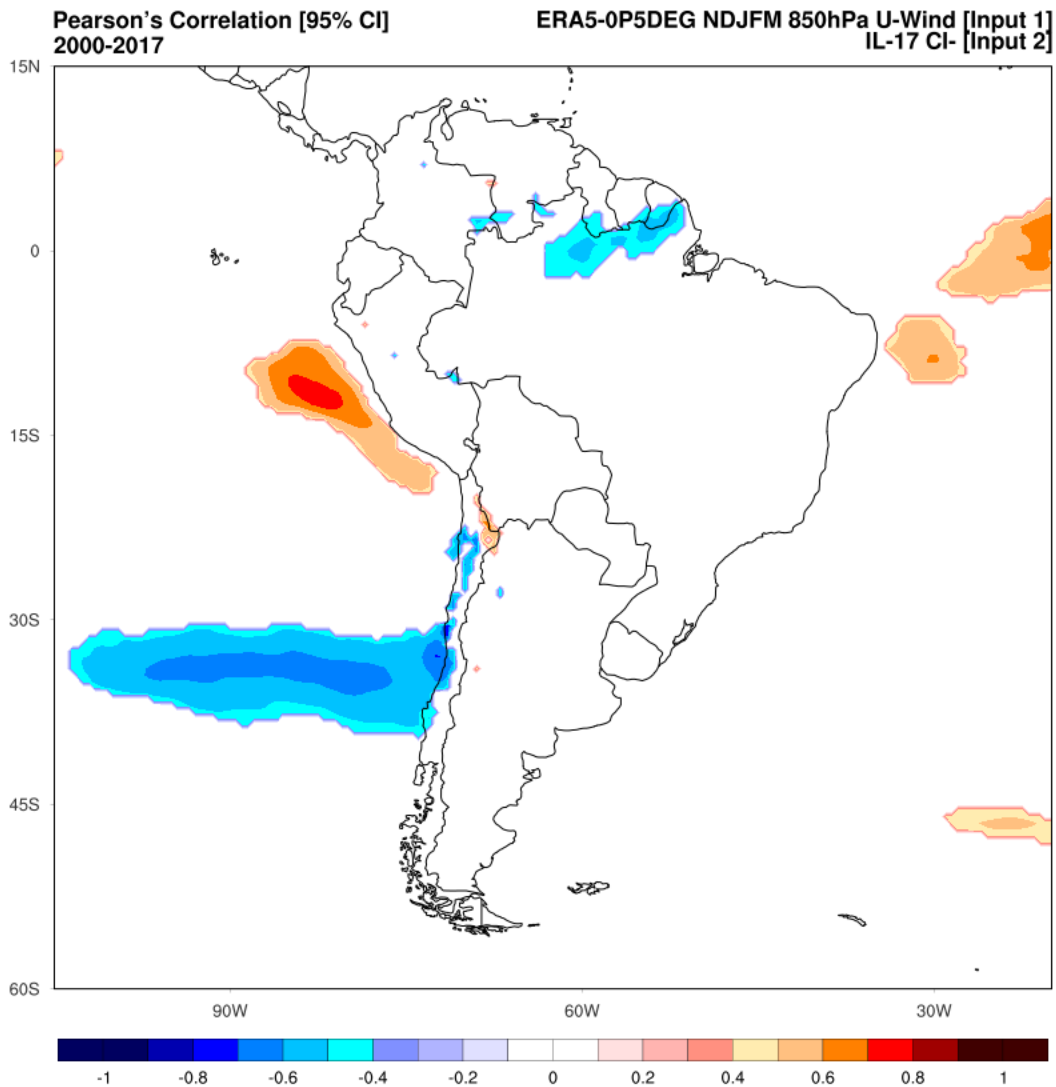
Figure S11. Pearson's correlation (95% CI) of ERA5 NDJFM 850hPa U-wind to IL-17 Cl⁻ record from 2000 to 2017. This map was generated by the University of Maine's Climate Change Institute data-visualization website Climate Reanalyzer (https://climatereanalyzer.org).

Figure S12. Pearson's correlation (95% CI) of ERA5 DJF 10-m wind speed to IL-17 Cd record from 2000 to 2017. This map was generated by the University of Maine's Climate Change Institute data-visualization website Climate Reanalyzer (https://climatereanalyzer.org).